Theor. Appl. Climatol. 61, 177–190 (1998)

Theoretical and Applied Climatology

[1] Department of Geography, Tel-Aviv University, Israel
[2] Israel Meteorological Service, Israel
[3] Department of Geophysics and Planetary Sciences, Tel-Aviv University, Israel

Spatial and Temporal Changes in Rainfall Frequency Distribution Patterns in Israel

T. Ben-Gai[1], **A. Bitan**[1], **A. Manes**[2], **P. Alpert**[3], and **S. Rubin**[2]

With 13 Figures

Received December 10, 1997
Revised June 24, 1998

Summary

Annual and monthly rainfall totals in Israel were analyzed to reveal any long term changes in their temporal and spatial distribution patterns, since the 1930s. The data consists of 60 *rainfall* stations, spread all over Israel from the far North to the Negev desert in the South, with long-term records of rainfall covering two normal periods. A gamma distribution function was fitted to the annual rainfall at each station for the two normal periods, and the shape and scale parameters of the distribution, as well as their percentage changes during the last normal period with respect to the first one, were analyzed.

The analysis of the annual distribution function parameters reveals some appreciable changes, that are statistically significant, in the spatial rainfall distribution patterns in the southern, northern and central parts of the country. The most striking feature is revealed in the South, where a more than 60 percent increase in the shape parameter occurs, and a similar rate of re-scaling, i.e. a decrease of about 40 percent in the scale parameter. Analysis of the monthly distributions revealed considerable changes in October and November, at the beginning of the rainfall season, and an appreciable change in March, at the end of the rainfall season.

1. Introduction

In many scenarios of future climate change, primarily due to the increase of greenhouse gas concentrations in the atmosphere, it is often assumed that only the mean (or the so-called "location" in an asymmetric distribution) would change, while the standard deviation remains unchanged. Hanson et al. (1988) examined how the frequency of certain extreme temperature events would change with increasing concentration of greenhouse gases in the atmosphere. They did so by allowing only the mean temperature to change, on the basis of the outcomes of General Circulation Model (GCM) numerical experiments.

It was shown, however, by Mearns et al. (1984), Katz (1991), and Katz and Brown (1992), that the relative frequency of extreme events is dependent on changes in the standard deviation, and not just the mean. Katz (1991) assumes that a change in a climate variable that possesses a probability distribution (possibly skewed in shape) will also result in a change in the shape of this distribution.

Our interest in local and regional changing patterns of the frequency distribution of rainfall, stems from the fact that the shape and dispersion of the frequency distribution may provide a clue as to how the probabilities of extremes will change if the mean changes (or not). Severe impacts on human activities, e.g., agricultural production and water management, may result from new extremes of rainfall, drought and flood, which are evident in the frequency distribution of rainfall rather than in its mean alone (Waggoner, 1989).

The idea of using probability distributions as a statistical paradigm for climate changes was recently suggested by Katz (1991). Accordingly, a climate change may involve a combination of two statistical outcomes: a shift in the location and a change in the scale of the distribution function.

The importance of changes in the spatial variability of rainfall is well illustrated in a recent study by Vinnikov et al. (1990). They have indicated that in spite of the total increase in rainfall over the USSR, the geographic and seasonal distribution was not favorable for crop production: the crop belt suffered from a severe agricultural drought, although the overall annual rainfall increased.

Israel is well known for its extreme spatial rainfall variability: over a few kilometers, rainfall isohyets may drop from 500 mm in the central coastal plain to 200 mm southward and eastward. Large amounts of annual rainfall in the northern part of the country feed the catchment area of the Sea of Galilee, which is the main fresh water reservoir in Israel. It is in this part of the country where rain amounts may reach values as high as 1200 mm per year. The rainy season in Israel lasts from September to April, with about 70% of the annual total falling during December, January and February. During the transitional seasons, when there is relatively strong convective activity, the temporal and spatial variability of rainfall is highest. Rainfall may be limited to a few days, but with extreme rainfall intensities, and may lead to disastrous results: flooding, damage to agriculture, and even loss of lives. It is thus obvious that climate change, either of a global or regional nature, may lead to changes in the spatial and temporal distribution of rainfall, with significant consequences for water resources and water management practices in Israel and elsewhere.

Revealing the nature of spatial and temporal changes in the frequency distribution of rainfall may provide an important tool to monitor possible changes in rainfall patterns, and their re-distribution. In the present study, the temporal and spatial changes in the frequency distribution of rainfall in Israel will be analyzed to identify any climate changes in rainfall distribution patterns, with due regard to extreme events at the lower and upper tails of the frequency distribution.

2. Methodology

Empirical histograms of rainfall totals over various time periods, and various climatic regions, may show a variety of shapes, from an exponential to a positively skewed, or close to normal distribution shape. In regions that have high amounts of rainfall, the mean has the highest frequency of rainfall and the distribution is close to normal (Vinnikov et al., 1990; Juras, 1994). In arid regions, variability is high with low amounts of annual rainfall in some years and high amounts in others. The frequency distribution of annual rainfall in arid regions will thus present an asymmetric shape with a long tail to the right (Hutchinson, 1990; Wilks, 1990; Katz, 1991).

The gamma distribution, being zero bounded provides a reasonably good fit to rainfall data, and has been widely used by many researche's (e.g., Mooley, 1973; Hutchinson, 1990; Ropelewski et al., 1985; Revfeim, 1985; Bradley et al., 1987; Hosking and Stow, 1987; Vinnikov et al., 1990; Waggoner, 1989; Villalpando et al., 1991; Wilks, 1989, 1990; Wilks and Eggleston, 1992; Juras, 1994; Ropolewsi and Halpert, 1996). It has, therefore, become a popular choice for fitting probability distributions to rainfall totals because its shape is similar to that of the histograms of rainfall data.

Fitting a theoretical distribution to rainfall totals makes it easy to estimate the frequency of rainfall amounts. Representative distribution parameters can be obtained from relatively short-term rainfall records, as short as 10 years in length (Revfeim, 1985).

Only a few studies of the frequency distribution of rainfall in Israel are available. According to Stanhill and Rapaport (1988), multi-year records of rainfall volume for the entire country fit a normal distribution quite well. However, according to Goldreich (1995), applying Gaussian statistics to annual rainfall data in Israel should be undertaken with some caution due to right skewed distributions, and the use of standard deviations to predict probable values (above or below a certain threshold) is not recommended.

2.1 Gamma Distribution

Many researchers, e.g., Thom (1958) and Wilks (1990), have discussed the general properties of the gamma distribution, and its application to meteorological parameters. According to Wilks (1990) it provides a flexible representation involving only two parameters. The probability density function for the distribution can be presented by the following equation:

$$f(x,\alpha,\beta) = \beta^{\alpha}\, x^{\alpha-1}\, e^{-\beta x}[\Gamma(\alpha)]^{-1} \quad \text{for}: \quad x \geq 0, \quad \alpha, \beta > 0 \tag{1}$$

Where: x – the random variable, i.e. rainfall total over the period of interest α – the shape parameter of the distribution expressing the extent of the symmetry around the mode (see Fig. 1).

β – the reciprocal of the scale parameter of the distribution in Eq. (1), scaling the rainfall amounts at respective frequencies. Lowering parameter β, i.e. increasing the scale parameter, means that the distribution function covers events with extreme rainfall amounts (see Fig. 1c and 1d).

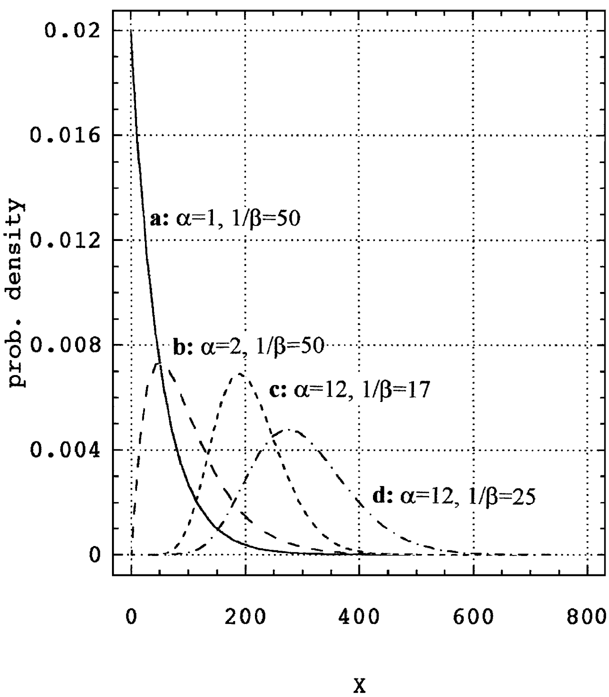

Fig. 1. Gamma distribution probability density. a: α=1, 1/β=50; b: α=2, 1/β=50; c: α=12, 1/β=17; d: α=12, 1/β=25

For $\alpha \leq 1$ – the density function has an exponential shape, with a maximum at $x = 0$ and is strongly skewed (Fig. 1a). Worthwhile noting, is that in arid and in semi-arid regions, with relatively small amounts of rainfall, the values of α may be less than 1.

For $\alpha = 1$ – the distribution function reduces to an exponential function special case at:

$$f = \frac{\beta e^{-\beta x}}{\Gamma(1)} \tag{2}$$

For $\alpha > 1$ – the distribution function in Eq. (1) will exhibit a single maximum at:

$$x = \frac{1}{\beta}(\alpha - 1) \tag{3}$$

The distribution function (1) will continue to exhibit skewness to the right (Fig. 1b), and only at relatively large values of, e.g., $\alpha > 20$, it will approach a normal distribution (Wilks, 1990).

It should be indicated that the value of x in (3) is identical to the "location" in the paradigm for climate change as suggested by Katz (1991).

The two moments of the distribution, the mean and the variance, are given by (Wilks, 1990):

$$\Gamma\,\text{mean} = \frac{\alpha}{\beta}; \quad \Gamma\,\text{variance} = \frac{\alpha}{\beta^2} \tag{4}$$

2.2 Estimating the Parameters of the Gamma Distribution

Basically there are two methods for the estimation of the parameters of the distribution: the shape parameter α and the scale parameter β. These are the methods of maximum likelihood (ML), e.g., Thom (1958), Choi and Wette (1969), Greenwood and Durand (1960), and the method of moments (M), e.g., Waggoner (1989) respectively. The method of moments has the advantage that it is applicable also for periods with zero rainfall, which might, obviously, be the case in arid and semi-arid regions. According to Thom (1958), however, the method of moments is not efficient for relatively small values of the shape parameter, which might be expected, particularly in arid and semi-arid regions such as those in Israel, and therefore, the ML method should be given preference.

In the present study the parameters of the gamma distribution for the annual rainfall amounts at all stations and the goodness of fit are estimated by the use of the STATGRAPHIC statistical Software Package, version 7.0 (Manugistics, Inc., Rockville, MD 20852–4999). The ML method is applied in this software package for the calculation of the distribution parameters. Of the two most commonly applied goodness-of-fit tests, the Chi-square test and the Kolmogorov-Smirnov one-sample test, preference was given to the Kolmogorov-Smirnov test (K-S). The advantage of the K-S test stems from its independence of the arbitrary selected rainfall classes. The significance of the fitted theoretical distribution was tested by the Kolmogorov-Smirnov significance test.

3. Data Base

The database for the present study consists of daily rainfall values from the Israel Meteorological Service rainfall network for the rainy seasons (October to May) covering a period of approximately 60 years, 1931 through 1990. To reveal climatic changes in the temporal and spatial distribution patterns of annual and monthly rainfall, the 60-years period was divided into two parts: 1931/32–1960/61 and 1961/2–1990/91. Due to missing data, mainly during the first period, only stations having at least a 20 year rainfall record for each period were used for this study. The gamma distribution was then fitted to the annual totals of rainfall at 60 rainfall stations possessing homogeneous long-

Table 1. *Rainfall Stations Sorted from North to South, and Gamma Distribution Parameters (see also Fig. 13)*

No	Station	X	Y	H,m	α(I)	α(II)	$1/\beta$(I)	$1/\beta$(II)	α PC	$1/\beta$ PC
1	Kefar Giladi	204	294	340	19.3	15.8	40.3	51.1	−19	26
2	Dafna	210	293	150	24.9	15.4	22.8	40.7	−39	78
3	Kefar Blum	207	286	75	17.7	14.1	29.6	38.0	−21	28
4	Eilon	171	274	300	25.5	14.1	30.8	55.7	−45	80
5	Miilya	174	269	500	20	16.3	37.8	49.7	−19	31
6	Ayelet	204	269	180	14.3	10.7	31.3	45.5	−26	45
7	Naharia	159	267	5	20.2	16.3	29.4	38.5	−20	30
8	Har Cnaan	197	264	934	24	12.9	31.3	55.6	−47	77
9	Kefar Hananya	189	260	410	22	19.4	35.7	40.0	−12	12
10	Akko	158	260	20	17.2	15.6	32.2	39.1	−10	21
11	Shefaram	166	245	150	16.9	19.8	30.8	30.9	17	0
12	Ramat Yohanan	161	244	58	17	17.7	31.2	31.6	4	1
13	Mizpe	198	243	75	13.6	17.4	30.3	25.6	27	−16
14	Yagur	157	238	30	19.6	17.3	35.9	41.7	−12	16
15	Deganya	204	235	−200	13.3	14.2	30.3	29.4	6	−3
16	Nazareth	178	235	460	12.4	17.1	51.0	36.2	37	−30
17	Kefar HaHoresh	176	234	430	11.9	15.9	49.0	37.0	33	−25
18	Tabor	188	234	140	16	13.5	32.3	43.5	−16	34
19	Atlit	144	233	10	17.6	12.4	27.7	42.6	−30	53
20	Ramat David	169	231	49	18.3	16.6	28.6	32.3	−10	12
21	Ginnnegar	174	230	100	14.2	15.1	37.0	33.3	6	−10
22	Sarid	171	229	110	18.1	17.3	28.6	31.3	−5	9
23	Mishmar Haemek	163	224	75	17	16.7	36.1	39.4	−2	9
24	Merhavya	179	223	60	15.6	17.8	27.8	25.6	14	−8
25	Zikhron Yaaqov	146	219	140	16.4	15.7	35.7	37.0	−5	3
26	Kefar Yehezqel	184	219	30	12.3	18.8	35.7	25.6	52	−29
27	Tel Yosef	187	218	5	10.7	15.2	38.5	28.6	42	−26
28	Sede Nahum	195	214	−105	10.4	14.9	33.7	24.1	43	−29
29	Hamadiya	199	214	−160	10.3	14.2	33.3	23.6	37	−30
30	Hefzi-Ba	190	213	−80	10.2	13.4	43.0	31.3	31	−28
31	Mesillot	194	211	−120	8.3	11.9	44.2	31.0	43	−30
32	Gan Shemuel	145	206	30	15.7	16.6	37.8	35.9	5	−6
33	Tirat Zvi	199	203	−220	8.4	11.9	34.8	23.6	41	−33

Table 1 (*continued*)

No	Station	X	Y	H,m	α(I)	α(II)	$1/\beta$(I)	$1/\beta$(II)	α PC	$1/\beta$ PC
34	Givat Hayim	143	200	25	11.6	15.5	53.1	37.9	33	−29
35	Ein HaHoresh	145	199	18	12.8	15.2	50.0	38.5	18	−23
36	Natanya	136	193	35	11.7	13.1	50.0	45.5	11	−9
37	Ramat HaKovesh	144	180	68	13.1	13.4	45.5	41.7	2	−9
38	Gan Hayim	140	179	40	13.8	15	41.7	41.7	8	0
39	Qiryat Shaul	133	170	40	13.3	13.6	41.7	43.5	2	4
40	Petah Tiqwa	138	166	50	11.2	14.2	50.0	45.5	26	−9
41	Miqve Israel	129	159	20	10.2	10.8	52.6	52.6	5	0
42	Lod	140	155	50	10.2	12	52.6	50.0	17	−5
43	Nezer Sireni	133	148	75	10.1	15.4	58.8	38.5	52	−35
44	Gan Shelomo	131	142	70	8.8	15.2	58.8	35.7	72	−40
45	Hulda	138	137	125	8.4	16.5	59.4	31.6	96	−47
46	Qiryat Anavim	161	135	700	8.4	14.9	81.8	47.5	77	−42
47	Hafez Hayim	131	133	80	7	13	66.7	41.7	85	−38
48	Jerusalem	171	132	815	8.8	13	55.6	45.5	47	−19
49	Beer Tuviya	124	127	55	6.7	10.6	71.4	52.6	58	−27
50	Kefar Menahem	134	126	125	6.3	12.2	71.4	40.0	93	−44
51	Beit Gimal	147	125	360	9.4	12.1	52.8	42.4	28	−20
52	Negba	119	118	90	7.4	10.5	64.8	45.5	41	−30
53	Beit Guvrin	140	113	270	8.6	12	41.7	37.0	39	−12
54	Gevaram	113	111	90	8.7	11.2	50.0	41.7	29	−17
55	Dorot	116	101	110	6.9	12.5	50.0	29.4	81	−42
56	Ruhama	122	100	180	6	10.4	55.6	34.5	73	−38
57	Beer Sheva	129	72	280	6.7	12.8	29.4	16.9	91	−43
58	Gevulot	99	69	135	7.9	10.8	20.4	16.4	36	−20
59	Revivim	123	50	290	5.5	7.9	18.5	14.9	43	−20
60	Mashabe Sade	129	45	344	5.3	7.7	18.9	15.6	45	−18

X, Y Coordinates in Israel net;
H,m – Station Elevation, meters MSL
α(I) – Shape Parameter, 1st normal Period; α(II) – Shape Parameter, 2nd normal Period;
$1/\beta$(I) – Scale Parameter, 1st normal Period; $1/\beta$(II) – Scale Parameter, 2nd normal Period
α PC – Percent Change of α, 2nd normal Period with respect to the first one.
$1/\beta$ PC – Percent Change of $1/\beta$, 2nd normal Period with respect to the first one.

term records as described above, and listed in Table 1.

The shape and scale parameters of the gamma distribution, for each station, and each of the two periods, are presented in Table 1. The goodness-of-fit of the theoretical gamma distribution to the empirical ones, for each station and each normal period, was then tested. Most of the fitted distributions have passed the K-S goodness-of-fit one-sample test at 0.05 significance level.

The statistical significance of the changes in the distribution parameters between the two periods were checked by two sample t test at the significance level of 0.05. The spatial distribution of the shape parameters for the two periods, as well as the percent changes of the values for the 25th, 50th, and 75th percentiles of the gamma distribution during the second period with respect to the first one, were then plotted.

4. Results

4.1 Changes in Annual Rainfall Distribution

A pronounced gradient of annual rainfall occurs in Israel from north to south. It was, therefore, of interest to investigate the behavior of the changes in the shape and scale parameters of the fitted gamma distribution to the annual rainfall data at stations sorted according to the north-southern direction (in order listed in Table 1). The results are plotted by histograms in Figs. 2, 3 and 4, respectively.

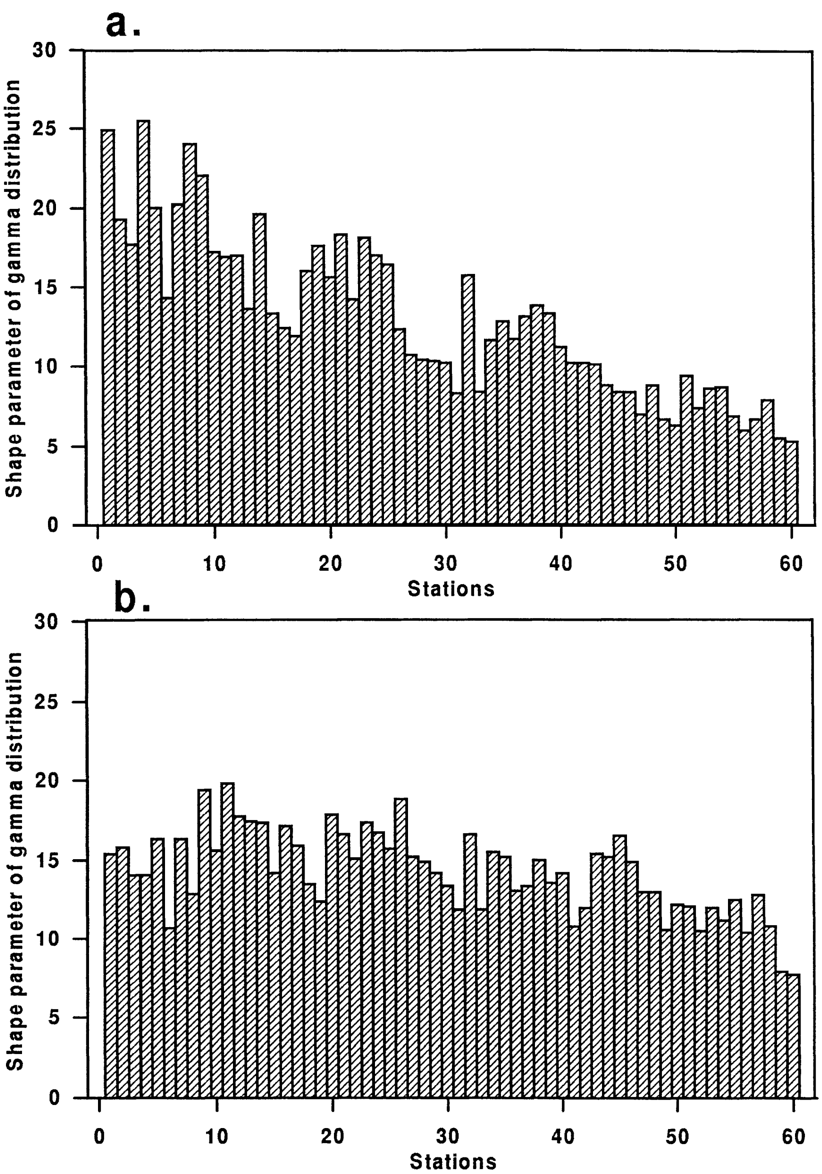

Fig. 2. Shape parameter for rainfall stations, sorted from north to south, (a) for the first period (1931–1960) and (b) for the second period (1961–1990)

The north-to-south decreasing trend of the shape parameter (Fig. 2a) during the first period (between 1931–1960) reflects the steep climatic gradients from the sub-tropical climate of northern Israel and the coastal plain, to the semi-arid and arid zones in southern Israel. This north to south trend of the shape parameter undergoes a striking change (Fig. 2b) during the second period (1961–1990). The previous trend is only weakly pronounced. A similar pattern, though opposite in nature, is exhibited by the scale parameter. During the first period, the scale parameter increased steadily from the north to the south (Fig. 3a), reflecting the increasing aridity towards the southern part of the country. The above pattern, however, changes during the second period, with no appreciable trend.

The above drastic changes in the north-south tendencies of the shape and scale parameters are well high highted by the percent changes of both distribution parameters during the second normal period with respect to the first one (Fig. 4a and 4b).

The spatial distribution of the shape parameter of the fitted gamma distribution for the two consecutive periods, as well as the percent change during the second period, with respect to the first one, are mapped in Figs. 5 and 6,

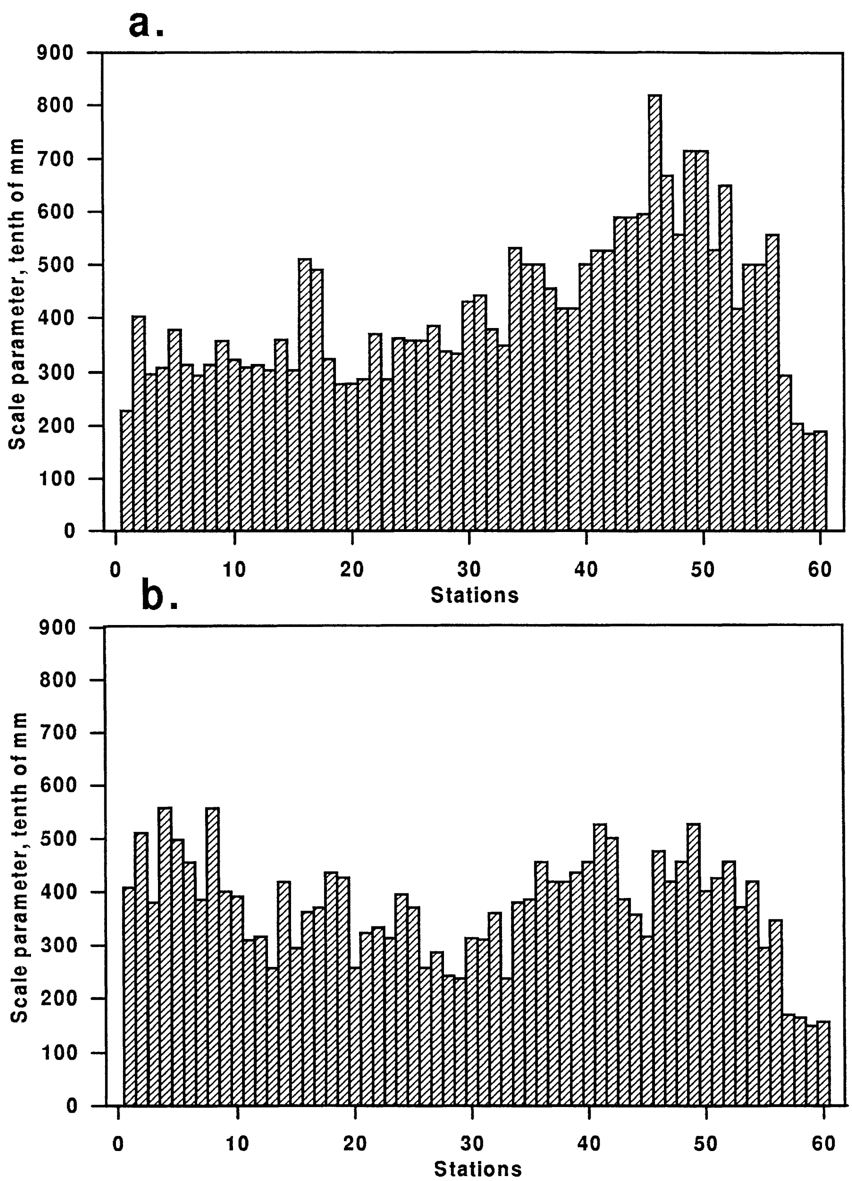

Fig. 3. As in Fig. 2, but for the scale parameter

respectively (see also Table 1). As can be seen, the shape parameters shows a negative trend in the northern part of Israel with a rather variable nature in the central part, and an overall positive trend in south. A similar pattern, though opposite in nature-positive in the north, variable in the central part, and negative in the south, is exhibited by the percentage change of the scale parameter in Fig. 7.

The changes in the spatial patterns of the shape and the scale parameters during the two consecutive periods may be indicative of a variety of factors which led to these rather peculiar patterns of change. These changes appear to be of a different nature in the north, the south and the central parts of the country, each part thus deserving separate treatment.

4.1.1 The North

An appreciable decrease occurs in the shape parameter, with a concurrent increase in the scale parameter in the far northern part of the country, including the Haifa region, in the second period,

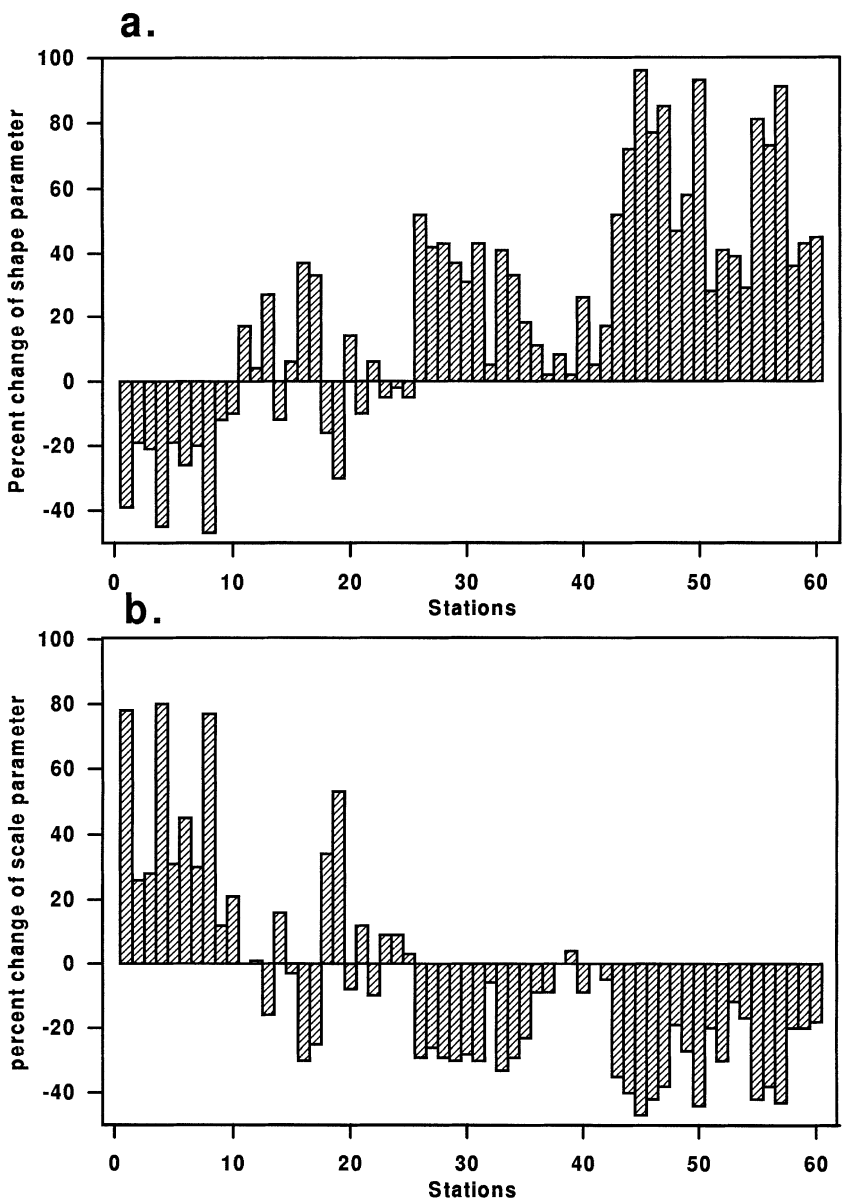

Fig. 4. Percent change of the fitted gamma distribution parameters during the second normal period with respect to the first one, for rainfall stations (sorted from north to south, as in Figs. 2 and 3)

compared to the first. These temporal changes are most distinctly expressed in Figs. 6 and 7. The changes were statistically tested and found to be significant at the level of 0.07.

The nature of the increase in asymmetry of the distributions in the North is due primarily to the "widening" of the upper tail of the distribution, as it becomes more positively skewed. This phenomenon is illustrated further by plotting the probability density function fitted to the annual rainfall amounts of Dafna, in the Northern part of Israel (see Fig. 13), for the two periods, shown in Fig. 8a. As can be seen, the distribution exhibits a positive shift of the location (towards higher rainfall values) and an increase in the width of the distribution. The thickening of the upper tail is indicative of an increased frequency of high extreme rainfall events during the second normal period. Analyzing the percent changes of the critical values during the second period with respect to the first one, corresponding to the 25th, 50th and the 75th percentiles respectively, elucidates this important conclusion further.

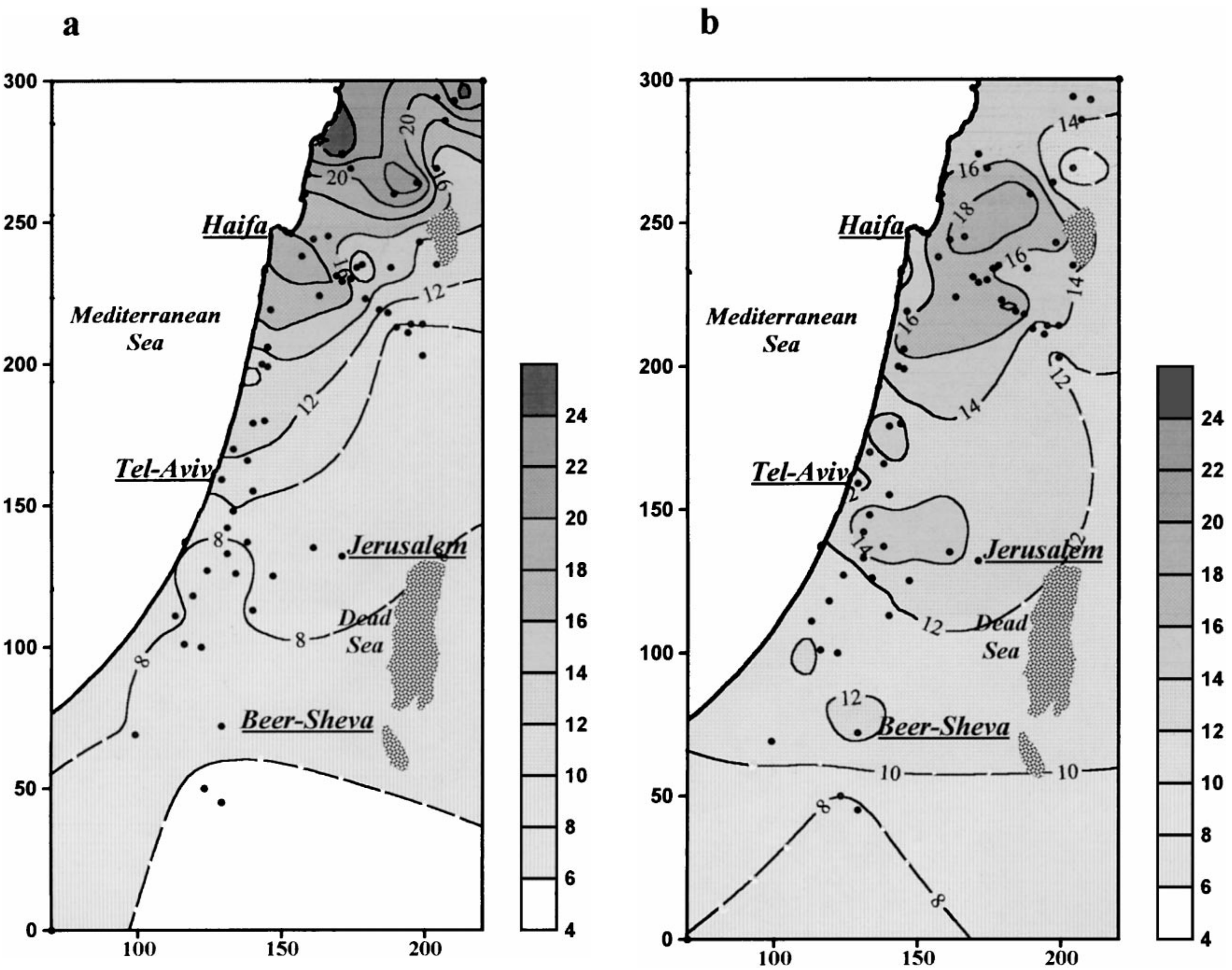

Fig. 5. Spatial distribution of the shape parameter for (a) the first period (1931–1960), and (b) the second period (1961–1990). Lines are dashed where extrapolation was done beyond these stations domain

The spatial distributions of the percent changes discussed above are mapped in Fig. 9 to 11. As can be seen, there is a slight decrease at the lower tail, and the same goes with the median value, with about a 10 percent increase of the critical values for the 75th percentiles during the second period.

4.1.2 The South

The most striking climatic change in rainfall frequency distribution, as reflected by the shape and scale parameter changing patterns, occurs in the southern part of the country. An increase in the shape parameter of more than 60 percent, and a decrease of about 30 percent in the scale parameter during the second period can be seen in Figs. 6 and 7. The changes of the distribution parameters were tested statistically and found significant at the level of 0.01. Both results are indicative of decreased aridity, with a distribution shape approaching normal. These results are in agreement with the results of previous studies by Otterman, et al. (1990), Ben-Gai et al. (1993, 1994), and Alpert and Mandel (1986).

These changes are illustrated by the changing patterns of the probability density curves of the gamma distribution fitted to the annual rainfall

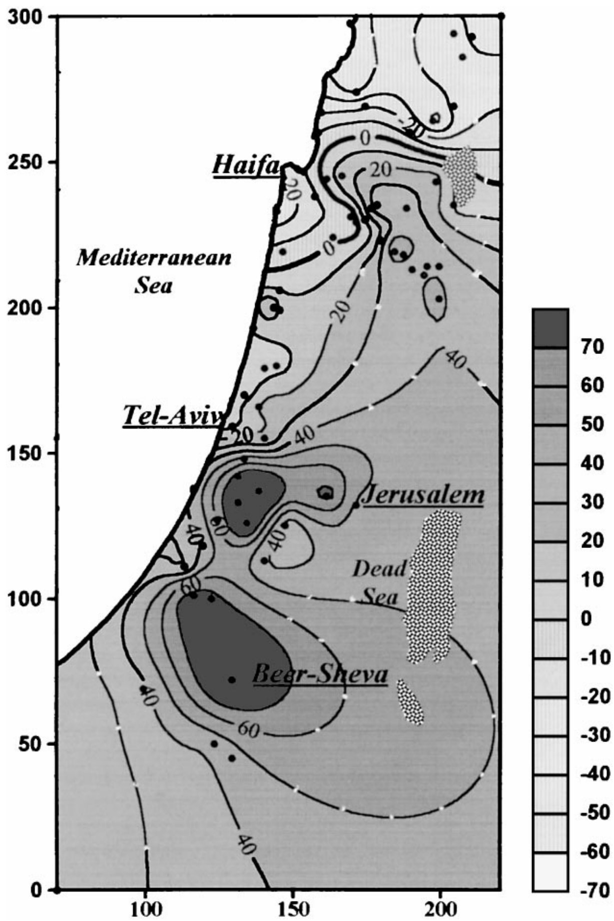

Fig. 6. Spatial distribution of the temporal change of the shape parameter. Values represent percent change between the two periods given by: $[(\alpha2\text{-}\alpha1)/\alpha1]^{*}100$

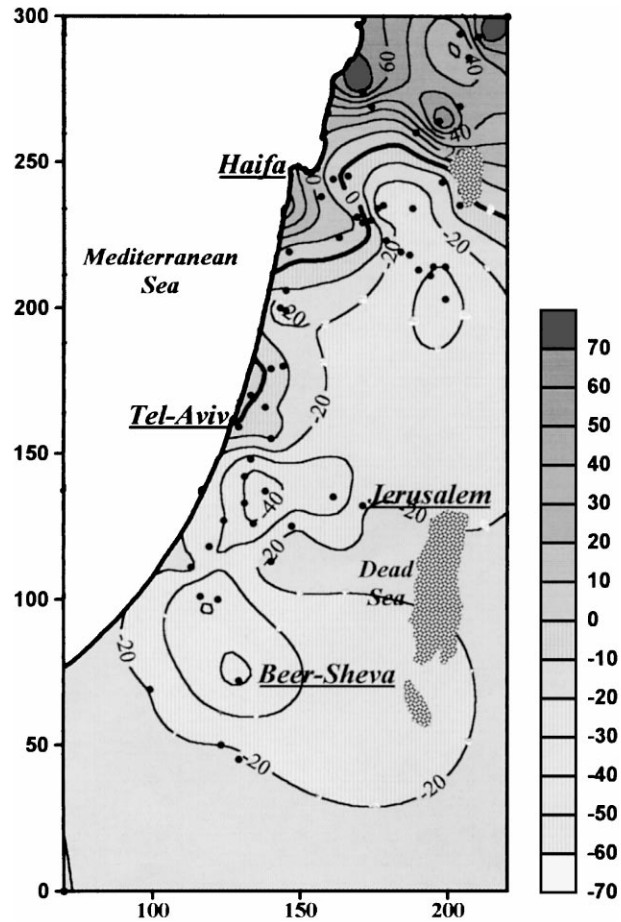

Fig. 7. As in Fig. 6, but for the scale parameter

amounts of Beer Sheva at the southern part of Israel (see Fig. 13), for the two periods, respectively (see Fig. 8b). The resulting climatic change in the South is evident also from the analysis of the critical values during the second normal period with respect to the first. The percent changes of the critical values are mapped in Figs. 9 to 11. They reveal a considerable increase in the lower percentiles, but only a moderate increase in the upper percentiles, thus showing a trend towards the normal distribution.

4.1.3 Central Israel

Examination of the percent change maps of the shape and scale parameters in Figs. 6 and 7 reveals a considerable increase in the shape parameter with a concurrent decrease in the scale parameter. The changes were tested statistically and found significant at the level of 0.01, except for the shape and scale parameter in the coastal plain north to Tel-Aviv which show smaller changes.

The probability density function fitted to the annual rainfall at two stations in central Israel is plotted in Fig. 8c and 8d. The station of Natanya (north of Tel Aviv, see Fig. 13 and Table 1) shows almost no change and the same applies to the percentiles. The station of Qiryat Anavim (west of Jerusalem, see Fig. 13 and Table 1), shows no change in the location, but reveals a narrowing of the shape of the distribution. In general, the percentile changes for this area show an increase in the lower tail and a considerable decrease in the upper tail, also showing a trend towards a normal distribution shape.

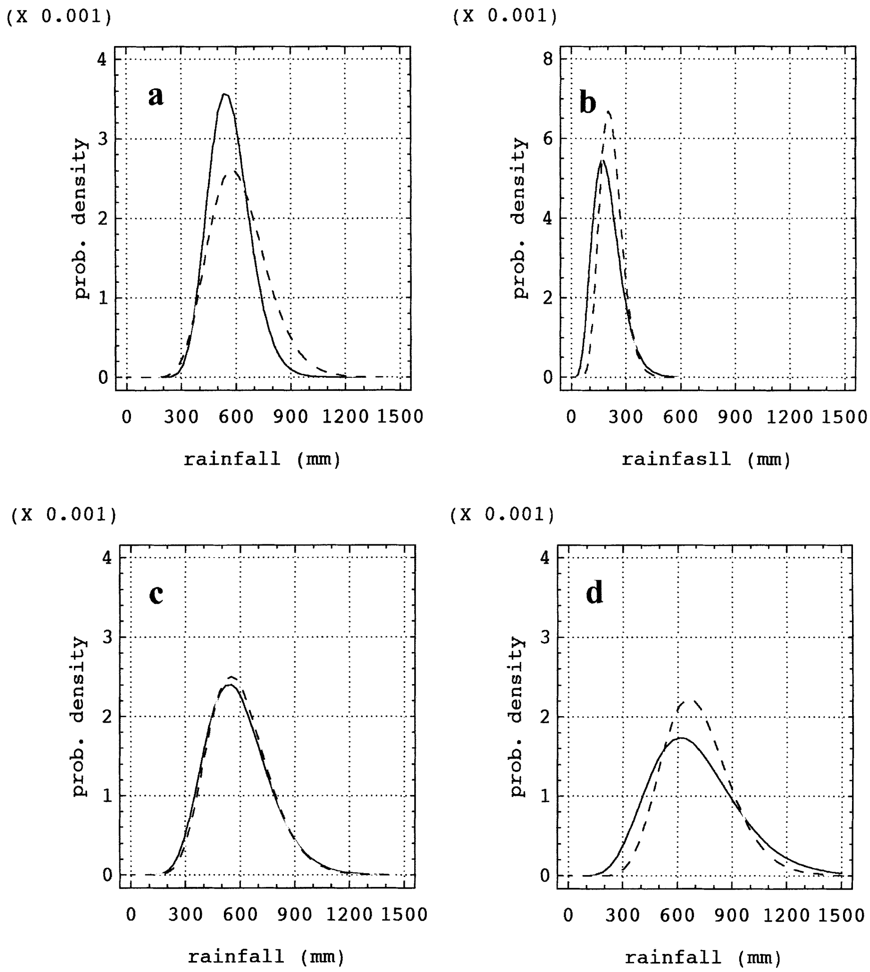

Fig. 8. Probability density function fitted to the annual rainfall stations in northern, southern and central Israel for the two normal periods. First period (full line), and second period (dashed line). Values are given in Table 1 and stations location in Fig. 13. Plots are for stations Dafna (a), Beer Sheva (b), Netanya (c) and Qiryat Anavim (d), corresponding to station numbers 2, 57, 36 and 46, respectively

4.2 Changes in Monthly Rainfall Distribution

The percent changes between monthly rainfall distribution of the shape parameter in the second period compared to the first in the north, south and central Israel are shown in Fig. 12. As can be seen, appreciable changes (statistically significant) are noticed in October and November all over Israel, at the beginning of the rainfall season and a striking change in March, at the end of the rainy season.

Among the main winter months (December to February), the changes are significant only in January, which shows a slight increase over the north and the central part of Israel which is significant (Fig. 12). The changes in March are the most important, since many stations that exhibited an exponential distribution in the first period with a shape parameter of $\alpha \leq 1$ (see Fig. 1a), show in the second period a different pattern: $\alpha > 1$, the distribution has a maximum, even though it continues to exhibit a tail to the right (see Fig. 1b).

5. Summary

A parametric statistical analysis of annual rainfall distribution in Israel over a period of 60 years, covering two 30-year periods, reveals some significant spatial and temporal changes in the shape and scale parameter patterns of the fitted gamma distribution. These changes have some important implications regarding the critical values at the upper tails of the distributions, and, consequently, the frequency of extreme rainfall events.

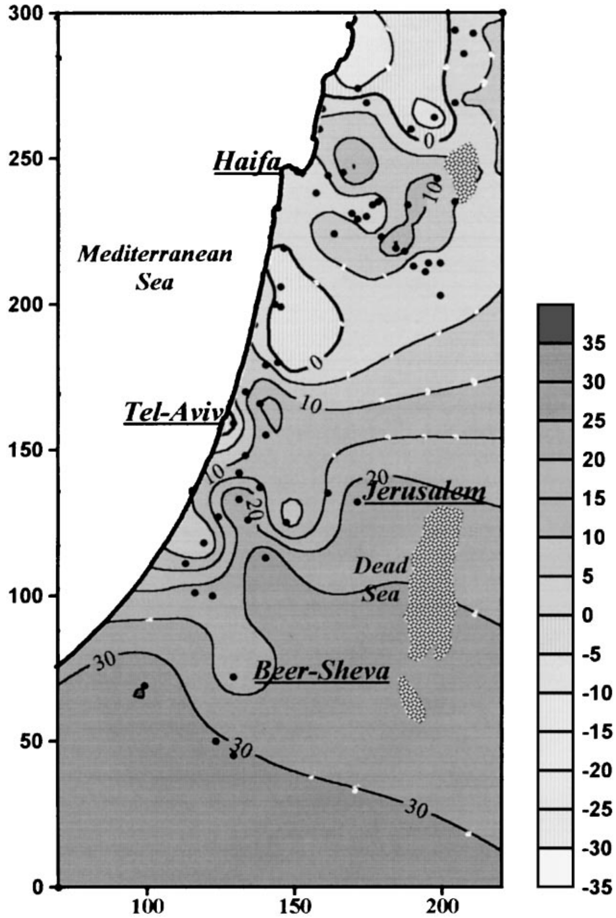

Fig. 9. Spatial distribution of the percent change of the critical values of 0.25 during the second normal period with respect to the first one

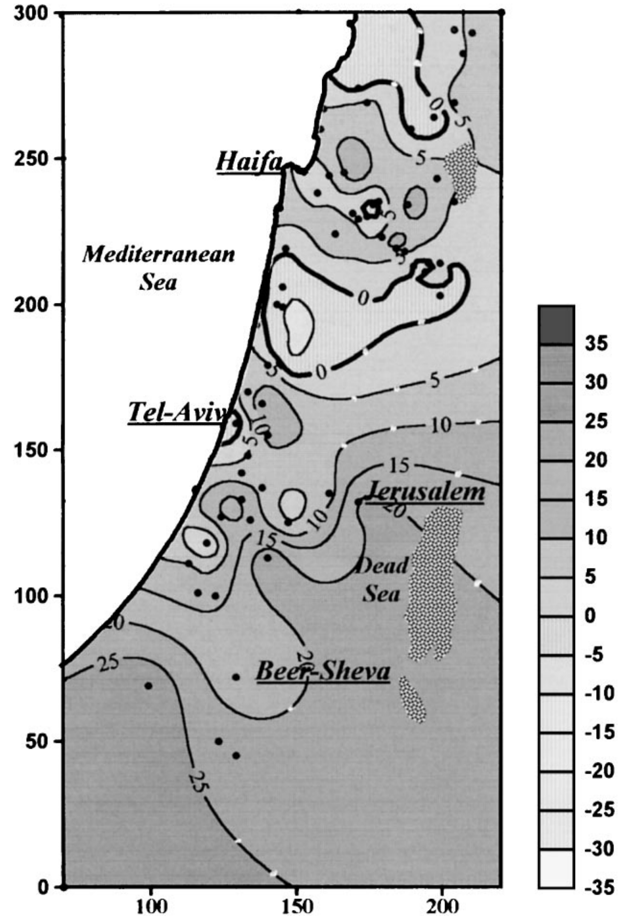

Fig. 10. As in Fig. 9, but for the critical values of 0.5 (median)

Although the possibility that some of these changes may reflect global changes in rainfall patterns can not be ruled out (Steinberger and Gazit-Yaari, 1996), the rather contrasting nature of these changes between the North and the South points towards the influence of regional factors.

The strongly increasing trend in the shape parameter, with the re-scaling negative trend in the south, can imply a retreat of aridity. The somewhat opposite changing patterns in the North, namely a decreasing trend in the shape parameter, with a concurrent increase in the scale parameter during the second period, are associated primarily with the thickening of the upper tail of the distribution. An increase in the critical values for the 75th percentiles is pronounced, with smaller changes in the median value and the lower tail critical values.

There is an increasing trend in the shape parameter, and a shift of location towards higher annual rainfall values, and the negative re-scaling trend in the central part of Israel. Monthly rainfall shape and scale parameters of the distribution show changes at the beginning and at the end of the rainfall season. The behavior of the North Atlantic Oscillation has recently been mentioned as a factor which could be responsible, at least partly, for changes in rainfall in the Middle East. There has been an attempt to trace possible teleconnections with rainfall anomalies in different parts of Israel to 13 different standarized teleconnections indices, compiled recently by the Climate Prediction Center of

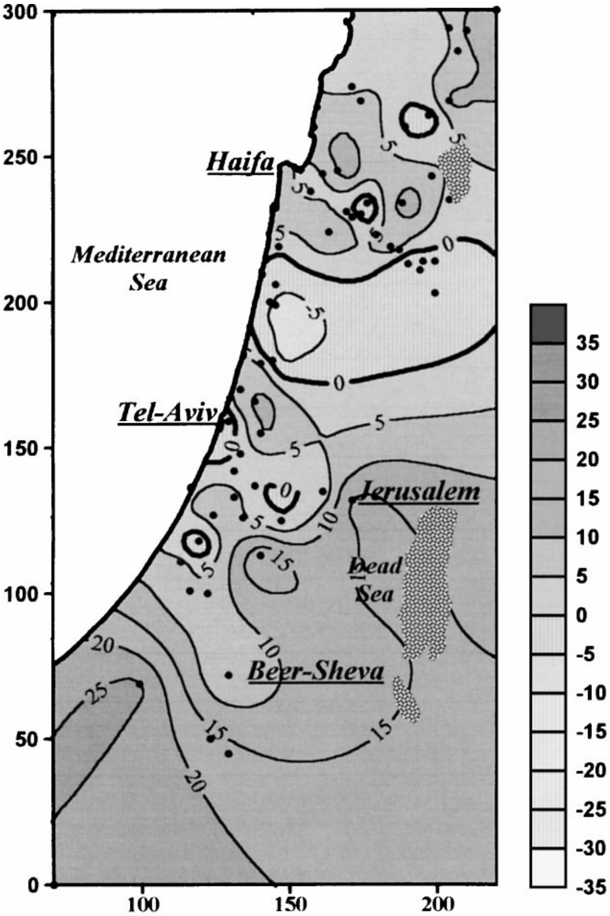

Fig. 11. As in Fig. 9, but for the critical values of 0.75

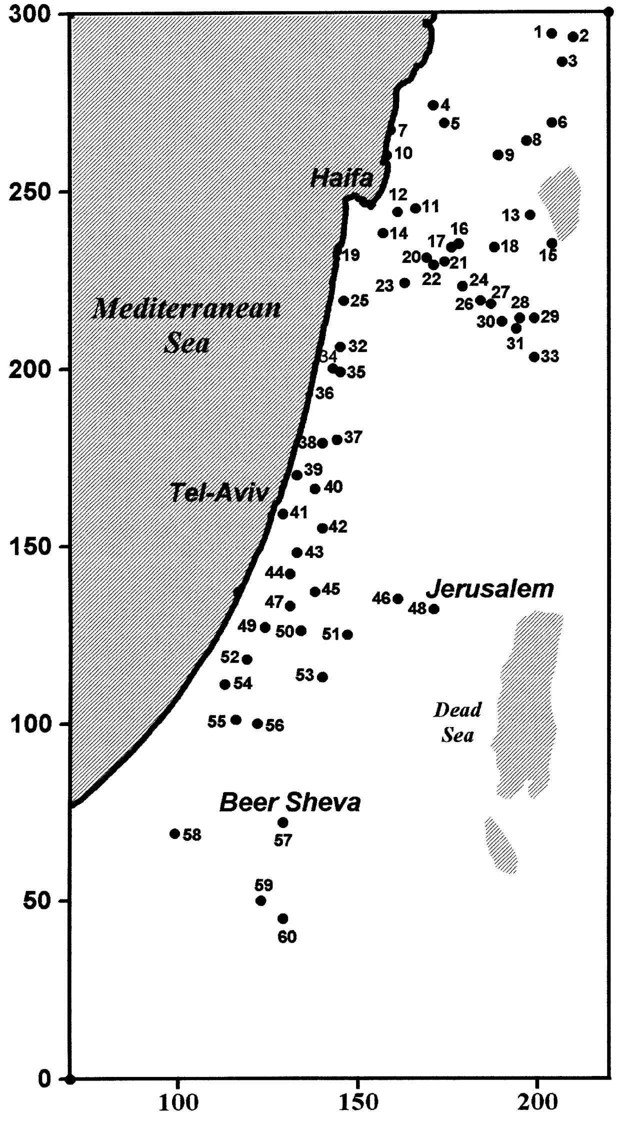

Fig. 13. 60 stations of the Israeli rainfall network. Stations are numbered as listed in Table 1, sorted from north to south

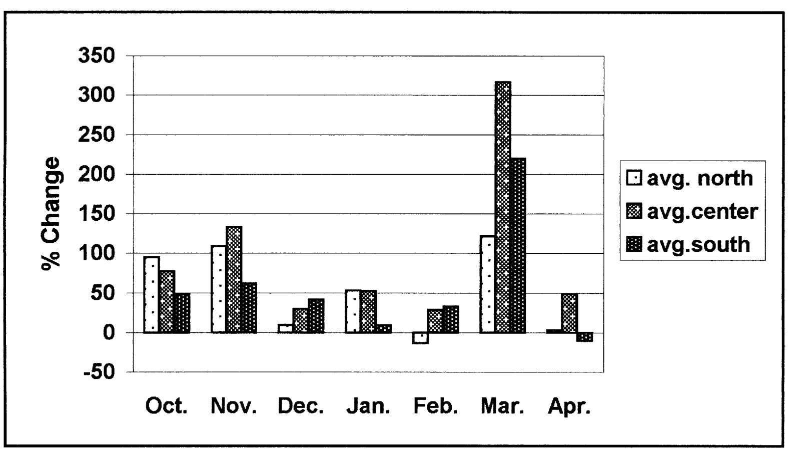

Fig. 12. Percent change in the shape parameter of average values of the fitted monthly distribution during the second normal period with respect to the first one from the northern, central and southern Israel

NOAA (USA), however, no statistically significant relationships were found.

References

Alpert, P., Mandel, M., 1986: Wind variability – an indicator for a mesoclimatic change in Israel. *J. Climate Appl. Meteor.,* **25**, 1568–1576.

Ben-Gai, T., Bitan, A., Manes, A., Alpert, P., 1993: Long-term change in October rainfall patterns in southern Israel. *Theor. Appl. Climatol.,* **46**, 209–217.

Ben-Gai, T., Bitan, A., Manes, A., Alpert, P., 1994: Long-term change in annual rainfall patterns in southern Israel. *Theor. Appl. Climatol.,* **49**, 59–67.

Bradley, R. S., Diaz, H. F., Eischeid, J. K., Jones, P. D., Kelly, P. M., 1987: Precipitation fluctuations over northern hemisphere land areas since the mid-19th century. *Science,* **237**, 171–175.

Choi, S. C., Wette, R., 1969: Maximum likelihood estimation of the parameters of the gamma distribution and their bias. *Technometrics,* **11**, 683–690.

Greenwood, J. A., Durand, D., 1960: Aids for fitting the gamma distribution by maximum likelihood. *Technometrics,* **2**, 55–65.

Goldreich, Y., 1995: Temporal variations of rainfall in Israel. *Clim. Res.,* **5**, 167–179.

Hanson, J., Fung, I., Lacis, A., Rind, D., Lebedeff, S., Ruedy, R., Russell, G., Stone, P., 1988: Global climate changes as forecast by Goddard Institute for Space Studies three-dimensional model. *J. Geophys. Res.,* **93**, 9341–9364.

Hosking, J. G., Stow, C. D., 1987: Ground-based, high-resolution measurements of the spatial and temporal distribution of rainfall. *J. Climate Appl. Meteor.,* **26**, 1530–1539.

Hutchinson, P., 1990: Frequency distribution of daily, monthly, seasonal and annual rainfalls in Somalia, and their use in the generation of rainfall distributions in data deficient areas. WMO Tropical Meteorology Research Program Report Series, No. **36**, Geneva, Switzerland, 239–245.

Juras, J., 1994: Some common features of probability distributions for precipitation. *Theor. Appl. Climatol.,* **49**, 69–76.

Katz, R. W., 1991: Towards a statistical paradigm for climate change. Preprints, 7th Conference on Applied Climatology, American Meteorological Society, Boston.

Katz, R. W., Brown, B. G., 1992: Extreme events in a changing climate: Variability is more important than averages. *Climate Change,* **21**(3), 289–302.

Mearns, L. O., Katz, R. W., Schneider, S. H., 1984: Extreme high-temperature events: Changes in their probabilities with changes in mean temperature. *J. Climate Appl. Meteor.,* **23**, 1601–1613.

Mooley, D. A., 1973: Gamma-distribution probability model for Asian summer monsoon monthly rainfall. *Mon. Wea. Rev.,* **101**, 160–176.

Otterman, J., Manes, A., Rubin, S., Alpert, P., Starr, D., 1990: An increase of early rains in southern Israel following land use change? *Bound.-Layer Meteor.,* **53**, 333–351.

Ropelewski, C. F., Halpert, M. C., 1996: Quantifying Southern Oscillation – Precipitation Relationships. *J. Climate,* **9**, 1043–1059.

Ropelewski, C. F., Janowiak, J. E., Halpert, M. S., 1985: The analysis and display of real-time surface climate data. *Mon. Wea. Rev.,* **114**, 1101–1106.

Revfeim, K. J. A., 1985: A note on the comparison of theoretical and empirical quantiles for monthly rainfall totals. *Atmos.-Ocean,* **23**, 414–419.

Stanhill, G., Rapaport, C., 1988: Temporal and spatial variation in the volume of rain falling annually in Israel. *Isr. J. Earth Sci.,* **37**, 211–221.

Steinberger, E. H., Gazit-Yaari, N., 1996: Recent changes in spatial distribution of annual precipitation in Israel. *J. Climate,* **9**, 3328–3336.

Thom, H. C. S., 1958: A note on the gamma distribution. *Mon. Wea. Rev.,* **86**, 117–122.

Villalpando, J. F., Biswas, B. C., Coulibaly, A., Gat, Z., Lomoton, B. S., Perry, K. B., Ulanova, E. S., 1991: Practical use of agromoteorological data and information for planning and operational activities in all aspects of agriculture, including farming systems. Final Report, WMO, Commission for Agricultural Meteorology, Geneva, 131 pp.

Vinnikov, K. Ya., Groisman, P. Ya., Lugina, K. M., 1990: Empirical data on contemporary global climate changes (temperature and precipitation). *J. Climate,* **3**, 662–677.

Waggoner, P. E., 1989: Anticipating the frequency distribution of precipitation if climate change alters its mean. *Agric. Forest. Meteor.,* **47**, 321–337.

Wilks, D. S., 1989: Rainfall intensity, the Weibull distribution, and estimation of daily surface run off. *J. Appl. Meteor.,* **28**, 52–58.

Wilks, D. S., 1990: Maximum likelihood estimation for gamma distribution using data containing zeros. *J. Climate,* **3**, 1495–1501.

Wilks, D. S., Eggleston, K. L., 1992: Estimating monthly and seasonal precipitation distributions using the 30- and 90-day outlooks. *J. Climate,* **5**(3), 252–259.

Authors' addresses: Dr. T. Ben-Gai, A. Bitan, Department of Geography, Tel-Aviv University, Israel; A. Manes, S. Rubin, Israel Meteorological Service; P. Alpert, Department of Geophysics and Planetory Sciences, Tel-Aviv University, Israel.